ELSEVIER

Biophysical Chemistry 109 (2004) 325–332

Biophysical Chemistry

www.elsevier.com/locate/bpc

Interpretation of concentration-dependence in aggregation kinetics

Masato Kodaka*

Institute for Biological Resources and Functions, National Institute of Advanced Industrial Science and Technology (AIST), Tsukuba Central 6, 1-1-1 Higashi, Tsukuba, Ibaraki 305-8566, Japan

Received 23 September 2003; received in revised form 1 December 2003; accepted 2 December 2003

Abstract

Aggregation processes are analyzed by two kinetic models, the random polymerization model and the nucleation-dependent polymerization model. A kinetic equation for the random polymerization model can be derived analytically, revealing the relation between the initial monomer concentration ($[M]_0$), the rate constant (k_a), time (t), the yield of detectable aggregate ($[F]$), and the critical aggregation number (m). However, time-course curves for the nucleation-dependent polymerization model can be obtained by numerical calculation. It is found that lag time (t_d) and half-time ($t_{1/2}$) are proportional to $[M]^{-1}$ in the random polymerization model, while t_d and $t_{1/2}$ are proportional to $[M_1]^{-s}$ ($1<s<n$; n is nucleus size) at the lower concentration and are less dependent on $[M_1]$ at the higher concentration in the nucleation-dependent polymerization model.

Keywords: Concentration-dependence; Random polymerization; Nucleation-dependent polymerization

1. Introduction

Aggregation processes are commonly observed in various fields. For instance, aggregation is indispensable in some proteins to exhibit specific functions. There are three forms of aggregation states in proteins; viz., amorphous states, crystals, and amyloid fibrils. Amyloid fibrils composed of β-sheet structures have been noted, since they are closely related to occurrence of conformational diseases. A typical example is amyloid-β-protein (Aβ), a causative compound of Alzheimer's disease (AD) with 39–42 amino acids, whose toxicity is well correlated with the formation of amyloid [1,2]. In the present study, two typical kinetic models are presented to describe aggregation processes. One is a model that all the species (monomers, oligomers, polymers) associate linearly and randomly to form detectable aggregate (fibrils), which is called here 'a random polymerization model'. The other is 'the nucleation-dependent polymerization model' in which individual monomers associate successively to form nuclei and then form fibrils [3,4]. Aggregation of Aβ is ordinarily analyzed on the basis of the nucleation-dependent polymerization model. In the previous study, detailed numerical calculation was carried out for the nucleation-dependent polymerization model and it was revealed that there are optimum values of the rate constants to give prominent

*Tel.: +81-29-861-6124; fax: +81-29-861-6123.
E-mail address: m.kodaka@aist.go.jp (M. Kodaka).

0301-4622/04/$ - see front matter © 2003 Elsevier B.V. All rights reserved.
doi:10.1016/j.bpc.2003.12.003

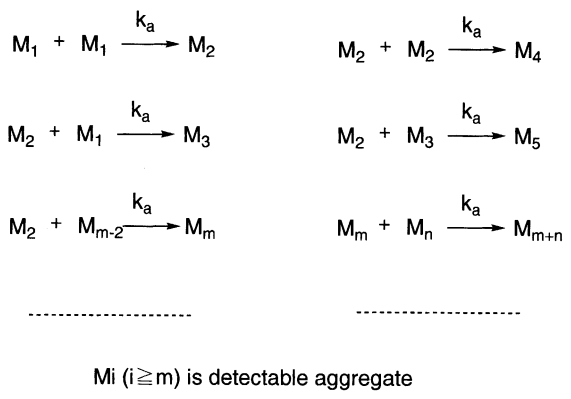

Scheme 1. Random polymerization model.

sigmoid curves [5]. Another important factor in the protein aggregation is the concentration-dependence of aggregation rate [6], that is, the relation between lag time (t_d) and concentration. Hofrichter et al. presented the empirical relation that t_d is proportional to c_t^{-z} (c_t: total initial protein concentration, z: number of molecules in nucleus) [4,7]. In the present study, the concentration-dependence of aggregation kinetics is examined by using the two models, viz., the random polymerization model and the nucleation-dependent polymerization model.

2. Calculation method

It is assumed that one monomer has two binding sites and, therefore aggregation proceeds linearly. There are two main ways in which monomers associate to form detectable aggregates (fibrils); a random aggregation and a nucleation-dependent aggregation. As shown below, the random polymerization model can be treated analytically, while the nucleation-dependent polymerization model can be solved by a numerical calculation.

2.1. Random polymerization model

First, the random polymerization model as shown in Scheme 1 is considered. In the case that the initial concentration of monomer is $[M]_0$ and fraction r of the total binding sites is already engaged in bonding, the total concentration ($[M]$) of all the species (monomer, oligomer, polymer) is given by Eq. (1).

$$[M]=[M]_0(1-r) \tag{1}$$

Since the parameter r also means the probability that one binding site is already engaged in bonding, the probability (P_i) that i-mer aggregate is formed is shown by Eq. (2),

$$P_i=r^{i-1}(1-r) \tag{2}$$

where r^{i-1} means the probability that $i-1$ bonds are formed and $1-r$ means the probability that the ith bond is not formed. Eqs. (1) and (2) give the concentration of i-mer aggregates as

$$[M]P_i=[M]_0r^{i-1}(1-\mathrm{r})^2 \tag{3}$$

Here the concentration of monomers incorporated into i-mer aggregate is represented by $i[M]P_i$. If the aggregates larger than $[m-1]$-mer are experimentally detectable such as fibrils, the concentration of monomer ($[F]$) included in the detectable aggregates is given by Eq. (4) in view of Eq. (3).

$$[F]=\sum_{i=m}^{\infty} i[M]P_i=[M]_0\sum_{i=m}^{\infty} ir^{i-1}(1-r)^2$$

$$=[M]_0r^{m-1}\{m-r(m-1)\} \quad (4)\ (\text{cf. Appendix A})$$

In the present study, the parameter m is termed as the critical aggregation number, which means the minimum size of detectable aggregates. Assuming that k_a is the rate constant of the bimolecular association, we obtain Eq. (5).

$$\mathrm{d}[M]/\mathrm{d}t=-k_a[M]^2 \tag{5}$$

Solving Eq. (5) under the initial condition of $[M]=[M]_0$ ($t=0$) results in Eq. (6).

$$[M]=[M]_0/([M]_0k_at+1) \tag{6}$$

Eqs. (1) and (6) lead to Eq. (7).

$$r=1-1/([M]_0k_at+1) \tag{7}$$

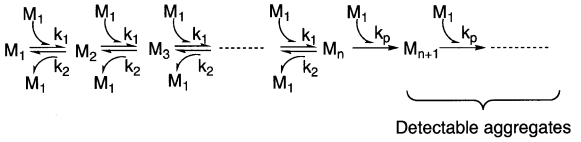

Scheme 2. Nucleation–dependent polymerization model.

Combination of Eqs. (4) and (7) gives Eq. (8).

$$[F]/[M]_0 = \{1-1/([M]_0 k_a t+1)\}^{m-1}\{1 + (m-1)/([M]_0 k_a t+1)\} \quad (8)$$

Eq. (8) is a general form representing the correlation among $[F]$, $[M]_0$, k_a, t and m.

2.2. Nucleation-dependent polymerization model

The second case is shown in Scheme 2, where a nucleus is formed before fibril formation. This is generally named as the nucleation-dependent polymerization model [3,4]. In this case, Eqs. (9)–(13) hold.

$$\mathrm{d}[M_1]/\mathrm{d}t = -k_1[M_1]\left(2[M_1]+\sum_{j=2}^{n-1}[M_j]\right) + k_2\left(2[M_2]+\sum_{j=3}^{n}[M_j]\right) - k_p[M_1]\left([M_n]+[N]\right) \quad (9)$$

$$\mathrm{d}[M_j]/\mathrm{d}t = k_1[M_1]([M_{j-1}]-[M_j]) - k_2([M_j]-[M_{j+1}]) \quad \{j=2-(n-1)\} \quad (10)$$

$$\mathrm{d}[M_n]/\mathrm{d}t = k_1[M_1][M_{n-1}] - k_2[M_n] - k_p[M_1][M_n] \quad (11)$$

$$\mathrm{d}[N]/\mathrm{d}t = k_p[M_1][M_n] \quad (12)$$

$$\mathrm{d}[F]/\mathrm{d}t = k_p[M_1]\{[N]+(n+1)[M_n]\} \quad (13)$$

The aggregates larger than n-mer is regarded as fibril, and $[N]$ and $[F]$ denote the number of fibrils and the total number of the monomer included in fibrils, respectively. Eqs. (9)–(13) are numerically solved under the initial conditions of $[M_j]$ ($j=1-n$), $[N]$ and $[F]$ by assuming appropriate values for rate constants, k_1, k_2 and k_p.

3. Results and discussion

Eq. (8) is the final analytical equation expressing the time course of the random polymerization model. Since $[F]/[M]_0$ is the function of m and $[M]_0 k_a t$, it is instructive to investigate the correlation among these quantities. Fig. 1 shows the typical relation between $\log t$ and $[F]/[M]_0$ for various $[M]_0$ values under $m=10$ and $k_a=1$. As predicted from Eq. (8), the individual curves are exactly superimposed by moving along the $\log t$ axis. Namely, when $[M]_0$ becomes 10^p times larger, the curve moves toward the negative side by p. Similar results are obtained for $m=5$ and 30 (figures not shown). Lag time (t_d) is generally noted, since it is a quantity characterizing sigmoidal aggregation curves [3,4]. Eq. (8) shows that t should be proportional to $[M]_0^{-1}$ when $[F]/[M]_0$, k_a, and m are constant. Actually, linear relation with the slope -1 is obtained between $\log[M]_0$ and $\log t_d$ as shown in Fig. 2. Eq. (8) also predicts that similar linearity with the slope -1 holds for the half-time ($t_{1/2}$) corresponding to $[F]/[M]_0 = 0.5$ (figure not shown).

The nucleation-dependent polymerization model (Scheme 2) provides sigmoidal time-course curves. Fig. 3 exhibits the typical relation between $\log t$ and $[F]/[M_1]_0$ for various $[M_1]_0$ values under nucleus sizes $n=10$, $k_1=1$, $k_2=100$ and $k_p=10\,000$ (arbitrary unit), in which the curves are shifted to negative side as $[M_1]_0$ becomes larger. Similar results are obtained for $n=5$ and 30 (figures not shown), where k_2 is 500 for $n=5$ and 5 for $n=30$. Fig. 4 shows the relation between $\log[M_1]_0$ and $\log t_{d,}$ in which t_d is available from Fig. 3. The noteworthy feature in Fig. 4 is that there is linear relation at the lower concentration for all the three nucleus sizes. The slope of the linear part become steeper as the nucleus size is increased from 5 to 30. Actually, the slope values are -2.4, -4.6 and -7.0 for $n=5$, 10 and 30,

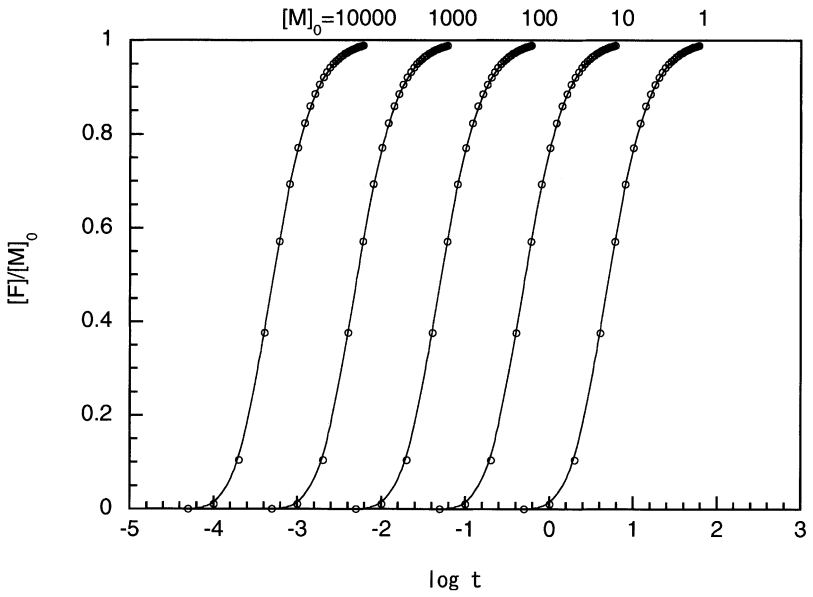

Fig. 1. Typical relationship between log t and $[F]/[M]_0$ in the random polymerization model: $m=10$, $k_a=1$: concentrations and rate constants are represented by arbitrary units.

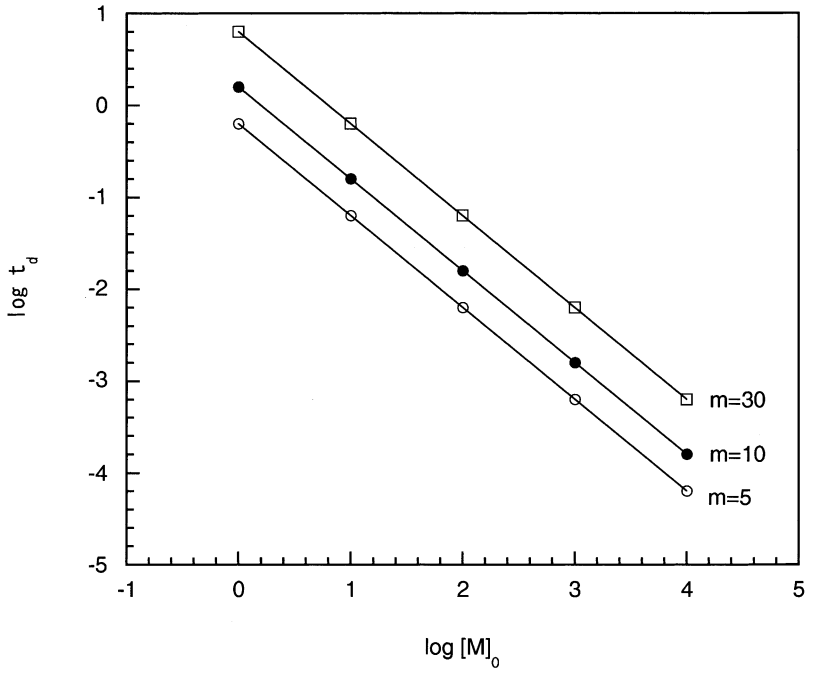

Fig. 2. Relationship between $\log[M]_0$ and $\log t_d$ in the random polymerization model: $k_a=1$: concentrations and rate constants are represented by arbitrary units.

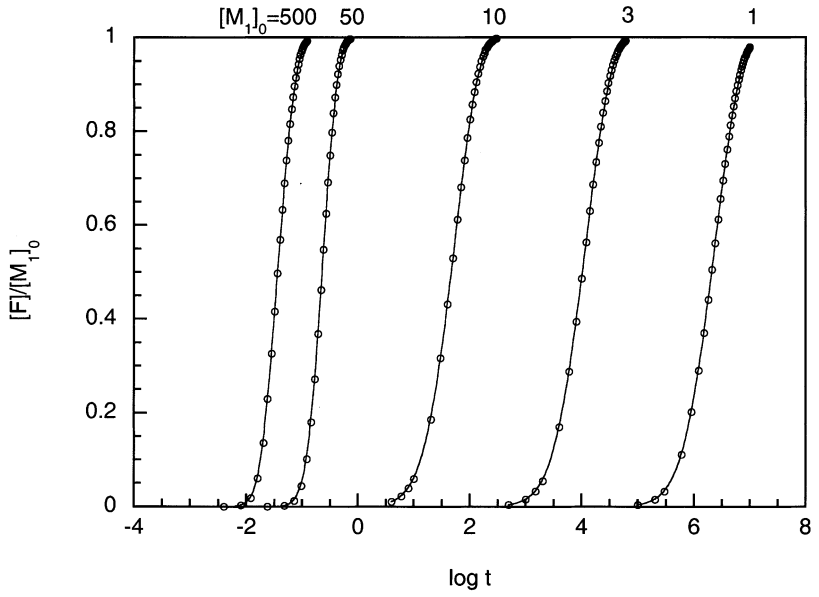

Fig. 3. Typical relationship between log t and $[F]/[M_1]_0$ in the nucleation-dependent polymerization model: nucleus size $n=10$, $k_1=1$, $k_2=100$, $k_p=10\,000$: concentrations and rate constants are represented by arbitrary units.

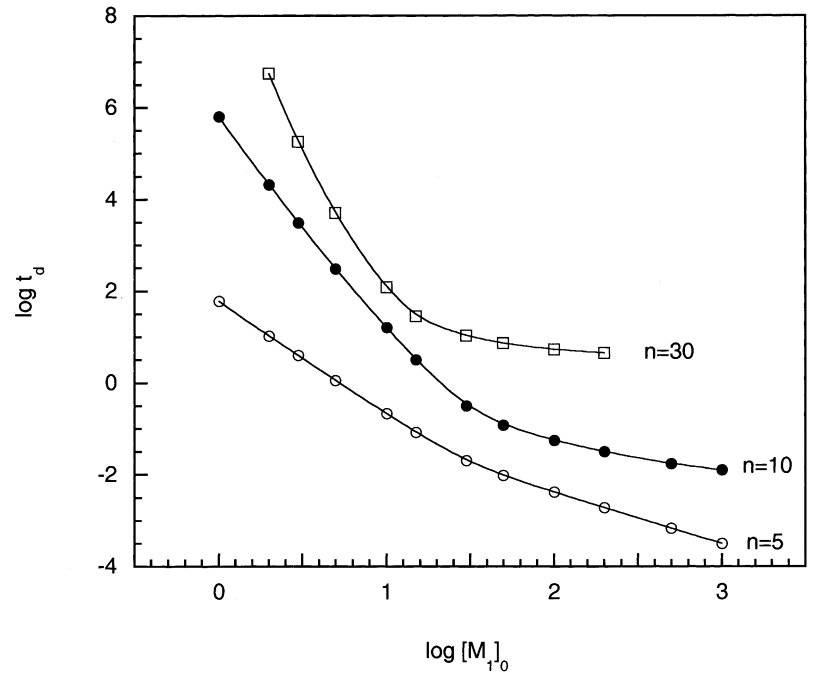

Fig. 4. Relationship between $\log[M_1]_0$ and $\log t_d$ in the nucleation-dependent polymerization model: $k_1=1$, $k_p=10\,000$, $k_2=500$ ($n=5$), 100 ($n=10$), 5 ($n=30$): concentrations and rate constants are represented by arbitrary units.

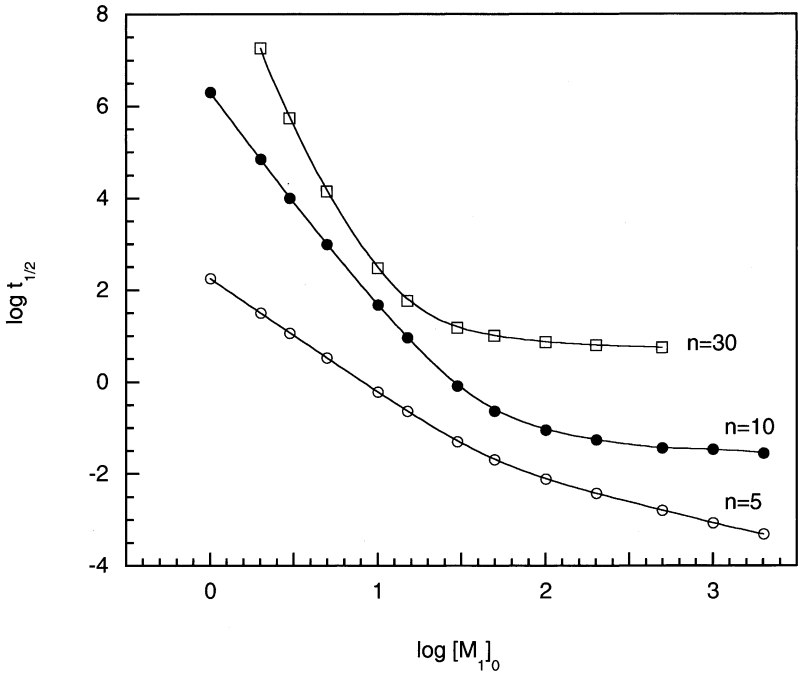

Fig. 5. Relationship between $\log[M_1]_0$ and $\log t_{1/2}$ in the nucleation-dependent polymerization model: $k_1=1$, $k_p=10\,000$, $k_2=500$ ($n=5$), 100 ($n=10$), 5 ($n=30$): concentrations and rate constants are represented by arbitrary units.

respectively. A similar result is obtained for $t_{1/2}$ (Fig. 5), in which the slopes are -2.5, -4.5 and -6.8 for $n=5$, 10 and 30. It is concluded, therefore, that t_d and $t_{1/2}$ are proportional to $[M_1]_0^{-s}$ ($s>1$) at the lower protein concentration in the nucleation-dependent polymerization model, which is in contrast to the random polymerization model that always gives $s=1$ as mentioned above. Fig. 6 illustrates the relation between n and s and clearly indicates the relation $1<s<n$, which is different from the idea of Hofrichter et al. that the parameter s represents nucleus size (n) [4]. This discrepancy is probably ascribed to the steady-state approximation in Hofrichter's treatment, while in the present study the exact calculation was carried out without such an approximation.

The present findings might serve to discriminate whether an aggregation mechanism is random or nucleation-dependent. It is instructive to compare the present calculated results and experimental findings. The linear relationship between the lag time ($\log t_d$ or $\log t_{1/2}$) and the protein concentration ($\log[M_1]_0$) as indicated in the lower concentration region of Fig. 4 or Fig. 5 is experimentally observed [4,7–11]. Notably, the s value is larger than unity in the lower concentration region but becomes smaller in the higher concentration region [10,11], which is well compatible with Figs. 4 and 5. From this comparison, some proteins are considered to aggregate in the nucleation-dependent polymerization manner rather than in the random polymerization mechanism. For instance, cold shock protein gives $s=2.1$ [8], deoxyhemoglobin S gives $s=\sim 30$ [4,7], and microtubules gives $s=2.9$ [9]. The decrease in the s value at the higher concentration predicted by Figs. 4 and 5 is experimentally observed by using deoxyhemoglobin S [10,11], though the tenth time ($t_{1/10}$) is used instead of t_d or $t_{1/2}$. Contrary to these proteins, there is a protein whose s value is very close to unity [12]. According to the present criteria, this small s value is attributable to either the random

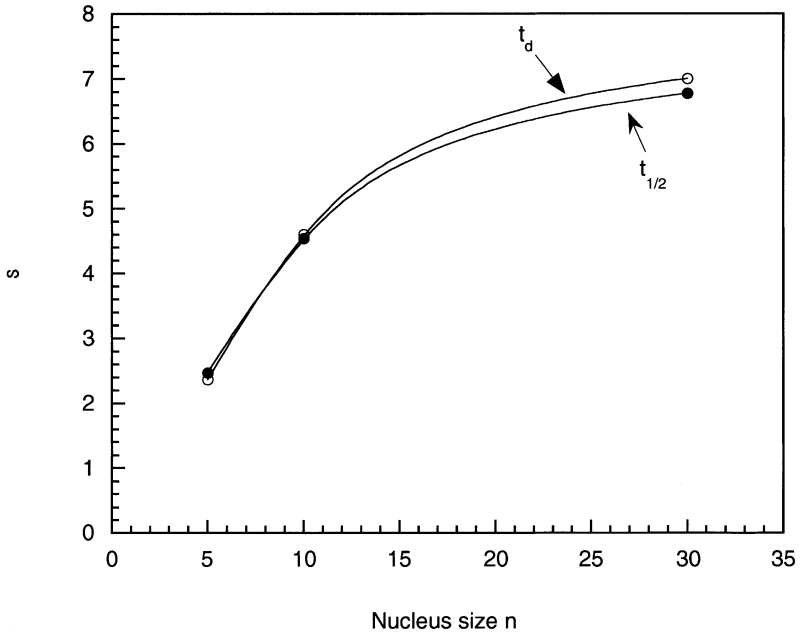

Fig. 6. Relation between n and s.

polymerization mechanism or the higher protein concentration in the nucleation-dependent polymerization model.

The present modeling study has revealed that the empirical equation proposed by Hofrichter et al [4] describes the behavior at lower protein concentration and that Fig. 4 affords the more general form.

Appendix A:

Eq. (4) can be derived as follows. The total concentration of monomers included in detectable aggregate is given by Eq. (A).

$$[F]=\sum_{i=m}^{\infty} i[M]P_i \qquad \text{(A)}$$

Substituting Eq. (3) into Eq. (A) yields Eq. (B),

$$[F]=[M]_0(1-r)^2\sum_{i=m}^{\infty} ir^{i-1}$$

$$=[M]_0(1-r)^2\left(\sum_{i=1}^{\infty} ir^{i-1}-\sum_{i=1}^{m-1} ir^{i-1}\right)$$

$$=[M]_0(1-r)^2(S_\infty-S_{m-1}) \qquad \text{(B)}$$

where $S_n=\sum_{i=1}^{n} ir^{i-1}$.

S_n term can be obtained in the following way. Eqs. (C) and (D) are easily obtained.

$$S_n=1+2r+3r^2+\cdots+nr^{n-1} \qquad \text{(C)}$$

$$rS_n=r+2r^2+3r^3+\cdots+(n-1)r^{n-1}+nr^n \qquad \text{(D)}$$

From Eqs. (C) and (D),

$$(1-r)S_n=1+r+r^2+r^3+\cdots+r^{n-1}-nr^n$$

$$=(1-r^n)/(1-r)-nr^n \qquad \text{(E)}$$

Thus,

$$S_n = (1-r^n)/(1-r)^2 - nr^n/(1-r) \quad \text{(F)}$$

Since $|r|$ is less than unity ($|r|<1$),

$$S_\infty = 1/(1-r)^2 \quad \text{and}$$

$$S_{m-1} = (1-r^{m-1})/(1-r)^2 - (m-1)r^{m-1}/(1-r) \quad \text{(G)}$$

Finally, combination of Eqs. (B) and (G) leads to Eq. (4).

References

[1] J.D. Sipe, A.S. Cohen, History of amyloid fibril, J. Struct. Biol. 130 (2000) 88–98.
[2] L.C. Serpell, Alzheimer's amyloid fibrils: structure and assembly, Biochim. Biophys. Acta 1502 (2000) 16–30.
[3] J.T. Jarrett, P.T. Lansbury, Seeding 'one-dimensional crystallization' of amyloid: a pathogenic mechanism in Alzheimer's disease and scrapie? Cell 73 (1993) 1055–1058.
[4] J. Hofrichter, P.D. Ross, W.A. Eaton, Kinetics and mechanism of deoxyhemoglobin *S* gelation: a new approach to understanding sickle cell disease, Proc. Natl. Acad. Sci. USA 71 (1974) 4846–4868.
[5] M. Kodaka, Requirements for generating sigmoidal time-course aggregation in nucleation-dependent polymerization model, Biophys. Chem., accepted.
[6] S.Y. Fung, C. Keyes, J. Duhamel, P. Chen, Concentration effect on the aggregation of a self-assembling oligopeptide, Biophys. J. 85 (2003) 537–548.
[7] J. Hofrichter, P.D. Ross, W.A. Eaton, Supersaturation in sickle cell hemoglobin solutions, Proc. Natl. Acad. Sci. USA 73 (1976) 3035–3039.
[8] A.T. Alexandrescu, K.J. Rathgeb-Szabo, An NMR investigation of solution aggregation reactions preceding the misassembly of acid-denatured cold shock protein A into fibrils, J. Mol. Biol. 291 (1999) 1191–1206.
[9] H. Flyvbjerg, E. Jobs, S. Leibler, Kinetics of self-assembling microtubles: an 'inverse problem' in biochemistry, Proc. Natl. Acad. Sci. USA 93 (1996) 5957–5979.
[10] F.A. Ferrone, J. Hofrichter, H.R. Sunshine, W.A. Eaton, Kinetic studies on photolysis-induced gelation of sickle cell hemoglobin suggest a new mechanism, Biophys. J. 32 (1980) 36–377.
[11] F.A. Ferrone, J. Hofrichter, W.A. Eaton, Kinetics of sickle hemoglobin polymerization I. Studies using temperature-jump and laser photolysis techniques, J. Mol. Biol. 183 (1985) 591–610.
[12] T. Arvinte, A. Cudd, A.F. Drake, The structure and mechanism of formation of human calcitonin fibrils, J. Biol. Chem. 268 (1993) 6415–6422.